

Controlling the dynamics of atomic correlations via the coupling to a dissipative cavity

Catalin-Mihai Halati,¹ Ameneh Sheikhan,² Giovanna Morigi,³ and Corinna Kollath²

¹*Department of Quantum Matter Physics, University of Geneva, Quai Ernest-Ansermet 24, 1211 Geneva, Switzerland*

²*Physikalisches Institut, University of Bonn, Nussallee 12, 53115 Bonn, Germany*

³*Theoretische Physik, Universität des Saarlandes, Campus E26, D-66123 Saarbrücken, Germany*

(Dated: April 1, 2024)

In this Letter, we report the onset of periodic oscillations of coherences in an interacting bosonic gas coupled to a resonator after a quantum quench. This dynamics extends the collapse and revival features of atomic correlations in optical lattices to a dissipative scenario and exhibits hallmarks of synchronization. The behavior emerges from the interplay of the quantum dissipative nature of the cavity field and the presence of a (approximate) strong symmetry in the dissipative system, providing a general recipe to engineer intriguing quantum dynamics. Additionally, we show that the approximate symmetry can arise dynamically during self-organization and can be employed to obtain long-lived coherences.

Open system control and measurement control have attracted an enormous interest in the last decade for the engineering of many body quantum systems [1–5]. Most proposals target the creation of interesting steady states, e.g. topological states of fermionic matter [6], non-trivial transport properties [7], quantum phases stemming from long-range spin interactions [8–12], or exhibiting dynamical synthetic gauge fields [13–18]. Much less attention has been devoted to the design of environments affecting the dynamical properties of a quantum system. In Ref. [19] we pointed out that it is extremely important for state engineering to consider the dynamics of correlations. For example, even though the BCS superconducting state itself can be targeted as a steady state by dissipation [20], the desired superconducting current-current correlations are not present as long as the dissipative coupling is applied [19].

In contrast, for isolated many body systems the dynamical features were in the spotlight in the last years. In this regard, an often employed scenario in ultracold atoms experiments is the quantum quench [21–25], e.g. in the observation of the collapse and revival of the matter wave field of a Bose-Einstein condensate [26]. In this experiment, a quench of the optical lattice potential was performed on a Bose-Einstein condensate and despite the presence of an extremely strong interactions a series of collapses and revivals of the coherence has been observed. The origin of the persistent oscillations of long-lived coherences could be associated with the interaction present between atoms and is therefore a many-body dynamical effect. Another proposed scenario in which persistent oscillations are present is due to a periodic Floquet driving [27, 28]. In such a situation, the so-called time crystal behavior has been observed [29–32], in which oscillations with a frequency different from the driving frequency arise.

In this work, we present a general recipe on how the interplay of dissipation and symmetries can be used in order to engineer intriguing dynamical phenomena in open quantum systems. We exemplify this by designing long lived synchronized coherences with a spatial structure for a system of interacting bosonic atoms coupled to an optical cavity. The realization of the long lived coherences relies on an intricate interplay between the dissipative state engineering and the pro-

tection of the dynamics by a strong symmetry, and it is related to purely imaginary eigenvalues of the Liouvillian operator, called rotating coherences [33]. The coupling between atoms and cavity determines which atomic correlations exhibit long-lived oscillations, and thus can become synchronized [34, 35], and which instead are damped rapidly by the dissipative coupling. In particular, for the chosen coupling, the coherences between sites at even distances exhibit long-lived oscillatory dynamics, while the coherences at odd distances are strongly suppressed (as sketched in Fig. 1(a)). We show that the quantum nature of the cavity field is essential in determining this dynamics and that the self-organization of the approximate symmetry can lead to a similar behavior.

One important element for understanding the dynamics of a dissipative system is the spectrum of the Liouvillian. For large dissipation rates Γ , the eigenvalues of the Liouvillian are clustered in bands, with gaps between the real parts proportional to Γ . An exemplary spectrum of the Bose-Hubbard model coupled to a dissipative cavity is shown in Fig. 1(b), determined using exact diagonalization (ED). Due to the direct dissipative coupling to the photon losses, most eigenstates of the Liouvillian have an eigenvalue whose real part is $\propto \Gamma$, e.g. in the subspaces marked with P_1 and P_2 , signaling an exponential decay of their contribution to the time evolution of the density matrix. However, in many-body and hybrid systems, the situation can be much more complex and eigenstates can exist with decay rates smaller than Γ , i.e. the states lying in the lowest subspace P_0 . The dynamics which takes place in P_0 is protected from the fast decay, since a direct coupling to dissipation is absent. Previous open system engineering [3] used often the decoherence free subspace Λ_0 (subspace of P_0), i.e. corresponding to vanishing real parts of the eigenvalues.

In the following, we show that in the considered scenario exciting possibilities arise to engineer dynamical features within the meta-stable subspace P_0 . By designing the dissipative coupling, here via the coupling to a lossy cavity, we can choose which dynamical features are rapidly suppressed (e.g., in Fig. 1(b) correlations probing the excited subspaces Λ_1 within P_0 , or $P_{n>0}$) and which are protected up to long times (with dynamics dominated by the lowest subspace Λ_0 within P_0). For example, in Fig. 1(b)-(c), the expectation

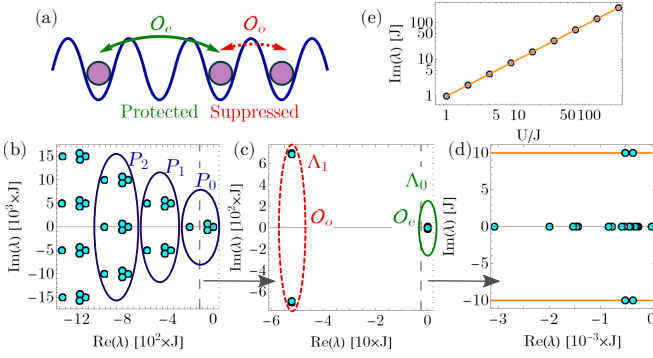


FIG. 1: (a) Sketch of ultracold atoms in an optical lattice potential. The operator \mathcal{O}_e probes the coherence between sites at even distance and \mathcal{O}_o at odd distance. (b)-(d) Eigenvalues spectra of the Liouvillian modeling the Bose-Hubbard model coupled to a dissipative cavity mode, Eqs. (1)-(2), obtained with ED for $L = 4$ sites, $N = 2$ particles, $\hbar\Omega\sqrt{N}/J = 1323$, $\hbar\delta/J = 5000$, $\hbar\Gamma/J = 750$, $U/J = 10$. We show the lowest (b) 1000 (c) 50 (d) 34 eigenvalues, where panels (c) and (d) are zoom ins of (b) and (c) at the right of the vertical dashed gray lines (as depicted by the gray arrows). We mark with P_n the subspaces containing n photonic excitations, with Λ_0 and Λ_1 the states corresponding to the decoherence free subspace and first excited subspace in the limit of vanishing J , respectively. The operator \mathcal{O}_e couples mainly to states in Λ_0 and \mathcal{O}_o to states in Λ_1 . (e) The dependence on the on-site interaction U of the imaginary part of the lowest eigenvalue whose imaginary part is in the range $[0.75U, 1.25U]$.

value of the operator \mathcal{O}_o will experience fast oscillations and a rapid decay to its steady state value, compared to \mathcal{O}_e , as it couples to an eigenstate with much larger magnitude of the real and imaginary parts, while still within the space P_0 .

Combining the dissipative nature with (approximate) strong symmetries gives another handle on the engineering of dynamical features. In the presence of a strong symmetry [33, 36], for which the generator commutes with both the Hamiltonian and the jump operators, the dynamics decouples in distinct symmetry sectors, each with its own steady or rotating states. In case one slightly breaks the strong symmetry [37], this generally reduces the number of steady states and gives rise to many slowly decaying states forming the subspace Λ_0 within P_0 . The decay timescale of this symmetry protected metastable states depends on the magnitude of the symmetry breaking term and can potentially be much smaller than the dissipative gaps of the Liouvillian in the presence of the strong symmetry. For example, the states shown in Fig. 1(e) would have zero real part in the limit $J = 0$, however, even at finite J their real parts are still much smaller than the ones corresponding to the states in Λ_1 .

We consider a one-dimensional lattice of interacting ultracold bosonic atoms inside a high finesse cavity. The dynamics of the system is given by a Lindblad equation for the density operator [38–42]

$$\frac{\partial}{\partial t}\rho = \mathcal{L}\rho = -\frac{i}{\hbar}[H, \rho] + \frac{\Gamma}{2}(2a\rho a^\dagger - a^\dagger a\rho - \rho a^\dagger a). \quad (1)$$

where a and a^\dagger are the annihilation and creation operators for the photon mode and the dissipation of the photons due to the imperfections of the mirror has strength Γ . The Hamiltonian H contains the terms

$$H_{\text{int}} = \frac{U}{2} \sum_{j=1}^L n_j(n_j - 1), \quad H_{\text{kin}} = -J \sum_{j=1}^{L-1} (b_j^\dagger b_{j+1} + \text{H.c.}),$$

$$H_c = \hbar\delta a^\dagger a, \quad H_{\text{ac}} = -\hbar\Omega(a + a^\dagger) \sum_{j=1}^L (-1)^j n_j. \quad (2)$$

H_{int} is the repulsive on-site interaction term of strength U , and H_{kin} the kinetic tunneling processes of the atoms with the amplitude J . The system is transversely pumped with a standing-wave laser beam, with δ the detuning of the cavity with respect to the pump beam. The period of the lattice is chosen to be twice the period of the cavity mode, such that the cavity mode effectively couples to the even odd density imbalance of the atoms, $\Delta = \sum_j (-1)^j n_j$, with the effective coupling strength Ω . Interacting bosonic models on a lattice coupled to an optical cavity have been realized experimentally in [43–45], while theoretical studies focused mostly on steady state properties [37, 41, 42, 46–58].

We analyze the quench scenario in which initially the atoms are in the Bose-Hubbard ground state and the atom-cavity coupling is suddenly turned on. We perform the exact time evolution of the master equation Eq. (1)-(2) using a recently developed method based on time-dependent matrix product states (tMPS) techniques (see Supplemental [59] and Ref. [60]). We further complement our understanding with analytical results in the limit of vanishing hopping J [59, 60] and ED for small systems. These approaches go beyond the often employed mean-field treatment of the cavity-atoms coupling [42]. In order to underline the effect of the cavity field, we contrast our results for the exact time-evolution of the atom-cavity system with the dynamics of a Bose-Hubbard model in the presence of a classical light field, i.e. a superlattice potential. The superlattice potential $V(t)$ can be obtained as a mean-field description of the coupled cavity-atoms dynamics, Eqs. (1)-(2), when the cavity is assumed to be a classical coherent state. The Hamiltonian in this situation is given by $H_{\text{MF}} = H_{\text{int}} + H_{\text{kin}} - V(t)\Delta$. For $V(t)$ we use a potential that corresponds at a mean-field level to the exact cavity dynamics (see Supplemental [59]), and we refer to it as the classical field approach.

Results in the presence of the approximate strong symmetry: We begin our analysis in the regime of vanishing atomic tunneling $J = 0$, where analytical results can be obtained, [59]. This is motivated by the fact that at $J = 0$ a strong symmetry arises in the model, as the local densities are conserved quantities, commuting with both the Hamiltonian and the jump operator [33, 36]. These results provide crucial information to our understanding also at small finite J , where the sectors of the symmetry are still a good approximate description. We show the ED spectra of \mathcal{L} in Fig. 1(b)-(d) for a small system. We note that the parameters used correspond to

a regime similar to the experiment performed in [44].

One can attribute the subspaces P_n , Fig. 1(b), to excitations on top of the photonic coherent state, for which the main contribution to the real part is given by $n\hbar\Gamma/2$ and by $\hbar\delta$ to the imaginary part. The subspaces with $n > 0$ show a fast decay and, thus, are important only for the short time dynamics. Therefore, we focus the analysis on P_0 , and in particular on the lowest two subspaces Λ_1 and Λ_0 , Fig. 1(c). In these subspaces the photon state is in a coherent state determined by the atomic density distribution. Λ_1 contains excited states capturing the coherence between different atomic distribution characterized by imbalances Δ and $\Delta \pm 2$. These coherences decay with a rate which depends, at large dissipation strength, inversely on Γ [59], as known from the Zeno effect. In contrast, Λ_0 is the decoherence free subspace, consisting of eigenstates with vanishing real part, which are protected by the strong symmetry for $J = 0$. As we detail in the Supplemental material [59], there are several types of states in Λ_0 , steady states of the form $\rho_{0,st} = |\alpha(\Delta); \{n_j\}\rangle \langle \alpha(\Delta); \{n_j\}|$, or traceless coherences $\rho_0 = |\alpha(\Delta); \{n_j\}\rangle \langle \alpha(\Delta); \{n'_j\}|$ between states with different density distribution and the same odd-even imbalance. In the case in which the latter describes a coherence between states with different interaction energies, the corresponding eigenvalue has a finite imaginary part (marked by the orange line in Fig. 1(d)). Such states are called rotating coherences and can lead to persistent synchronized oscillations in the long-time limit [33–35]. We checked the dependence of the imaginary part on U for the ED results for small J in Fig. 1(e), recovering the linear dependence expected for $J = 0$.

We observe that a finite J , smaller than the $J = 0$ gap between Λ_1 and Λ_0 , induces a finite real part to all eigenvalues, except one, lying in Λ_0 (see Fig. 1(d)). This marks the transition from multiple steady states due the strong symmetry to a single steady state in absence of the symmetry. The slight breaking of the symmetry creates a subspace of long-lived metastable states only weakly coupled to dissipation, which dominate the long-time dynamics, as we see in the time-evolution of the atomic correlations, Fig. 2(a)-(b) (same parameters as in Fig. 1(b)-(e)). Here we depict the time-evolution of the single particle correlations, $\text{Re}\langle b_4^\dagger b_{4+d} \rangle$, obtained with the tMPS based approach of simulating Eqs. (1)-(2), for a larger system (see Supplemental [59]). For odd distances d the single particle correlations probe the evolution of the states contained in Λ_1 , while for even distances d the states in the subspace Λ_0 are probed. We observe extremely different timescales for odd and even correlations, which reproduce very well the dynamics we aimed to engineer and characterized in terms of the approximate strong symmetry. At even distances the single particle correlations show oscillations (Fig. 2(a)), whose frequencies are determined by the value of U (red points and line in Fig. 2(e)). The oscillations are only weakly damped on the timescale of atomic hopping J . In contrast, for odd distances both the frequencies of the oscillations and their exponential decay to a small value occur

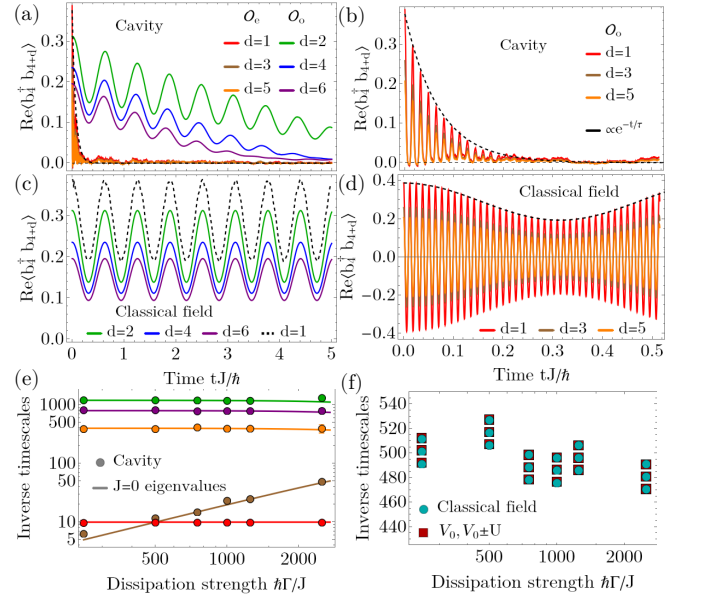


FIG. 2: Time evolution of the single particle correlations $\text{Re}\langle b_4^\dagger b_{4+d} \rangle$, for the (a)-(b) dissipative quantum description of the cavity (Eqs. (1)-(2)) and (c)-(d) classical field approach, for $\hbar\Omega\sqrt{N}/J = 1323$, $\hbar\delta/J = 5000$, $\hbar\Gamma/J = 750$, $U/J = 10$, $N = 7$, $L = 14$. The dashed black curve in (a) and (b) represents an exponential fit of the decay of the maxima for $\text{Re}\langle b_4^\dagger b_5 \rangle$. The dashed black curve in (c) and (d) represents the interpolated behavior of the maxima of $\text{Re}\langle b_4^\dagger b_5 \rangle$ for the classical field case. (e) Inverse timescales for dissipative quantum dynamics, the points correspond to data extracted from the tMPS evolution and lines to the $J = 0$ eigenvalues [59], with red $|\text{Im}\lambda_0| = U$, brown $|\text{Re}\lambda_1| = \frac{2\hbar\Omega^2\Gamma}{\delta^2 + \Gamma^2/4}$, and $|\text{Im}\lambda_1| = \frac{4\hbar\Omega^2\delta}{\delta^2 + \Gamma^2/4}(1 - \Delta)$ in green ($\Delta = 7$), purple ($\Delta = 5$) and orange ($\Delta = 3$). (f) Inverse timescales for classical field dynamics, extracted from the numerical simulations with circles and the late time value of the potential $V_0 = V(t \approx 5)$ and $V_0 \pm U$ with squares.

on much faster timescales (Fig. 2(a)-(b)). We extract these timescales and we see very good agreement with the analytically computed eigenvalues corresponding to Λ_1 in Fig. 2(e) (brown for the decay rate and green, purple and orange for the frequencies of the oscillations). We note that at $J = 0$ the synchronized oscillations are related to the fact that the operators $b_i^\dagger b_{i+d}$, for d even, can be used to construct the eigenstates with purely imaginary eigenvalues [34, 35, 59].

Furthermore, the importance of the dissipative quantum nature of the cavity field is highlighted by the comparison with the case of a classical field realizing a superlattice potential H_{MF} , (Fig. 2(a)-(b) in contrast to Fig. 2(c)-(d)). For the single particle correlations at even distances the oscillation frequency is the same for both the quantum and classical case, given by U , but in the case of the classical potential the oscillations do not show an attenuation up to the times shown (Fig. 2(c)). For odd distances the difference in behavior is even more striking, for the classical field the frequencies of the oscillations are given by the height of the potential and

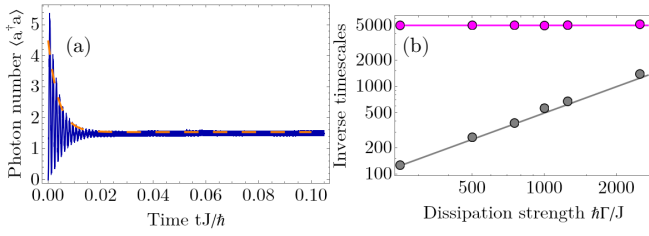


FIG. 3: (a) Time evolution of the photon number (Eqs. (1)-(2)). Dashed orange line corresponds to an exponential fit of the decay of the short time oscillations, with a decay rate $\tau^{-1}/J = 261 \pm 12 \approx \hbar\Gamma/2J$. (b) The frequency (magenta) and decay rate (gray) of the short time oscillations of the photon number versus $\hbar\Gamma/J$, the points are extracted from the tMPS simulations and the lines are given by $|\text{Re } \lambda_{P_1}| = \hbar\Gamma/2$ and $|\text{Im } \lambda_{P_1}| = \hbar\delta$. Parameters used are $L = 14$, $N = 7$, $\hbar\delta/J = 5000$, $U/J = 10$, (a) $\hbar\Omega\sqrt{N}/J = 6614$, $\hbar\Gamma/J = 500$, (b) $\hbar\Omega\sqrt{N}/J = 1323$.

on-site interactions (as shown in Fig. 2(d)-(e)), and the oscillations do not decay up to long times (dashed black line in Fig. 2(c)). Thus, the suppression of the correlations at odd distances is due to the open quantum nature of the cavity field and cannot be explained at a mean-field level by a classical superlattice potential.

Photon number dynamics: An interesting question is what timescales are reflected in the relaxation behavior of the photon number. We observe in Fig. 3(a) that after an initial fast increase the photon number exhibits damped oscillations and afterwards maintains a fairly constant value. The frequency of the oscillations is consistent with the value of the detuning δ and the observed fast decay with the inverse timescale of $\Gamma/2$ (see Fig. 3(b) and [59]), corresponding to the subspace P_1 in Fig. 1(b). We note that the photon number has not reached the steady state for the latest time shown in Fig. 3(a), the long time dynamics corresponds to timescales set by the subspace Λ_0 . Additional information can be obtained by investigating the single quantum trajectories sampled in our numerical method. The photon number indicates that the trajectories are projected quickly to subspaces spanned by states with the same imbalance Δ (shown in the Supplemental [59]). These results can be interpreted in connection with the phenomenon of dissipative freezing for the case of an approximate strong symmetry [37, 61, 62].

Cavity-induced self-organized synchronization: Up to this point we made the connection between the timescales observed in the single particle correlations and the eigenvalues of the Liouvillian for small J in the regime of large detuning and dissipation. Next, we show that even in regimes initially far from the strong symmetry, due to the self-organization of the cavity-atom system, an approximate symmetry arises which again protects synchronized long lived coherences. This can be understood since up to zero order, the effect of the cavity field is to create a deep superlattice for the atoms which suppresses tunneling and restores effectively the symmetry. In order to show this, we take the very challenging regime in which all the parameters are comparable, e.g $\hbar\Gamma/J = 1$,

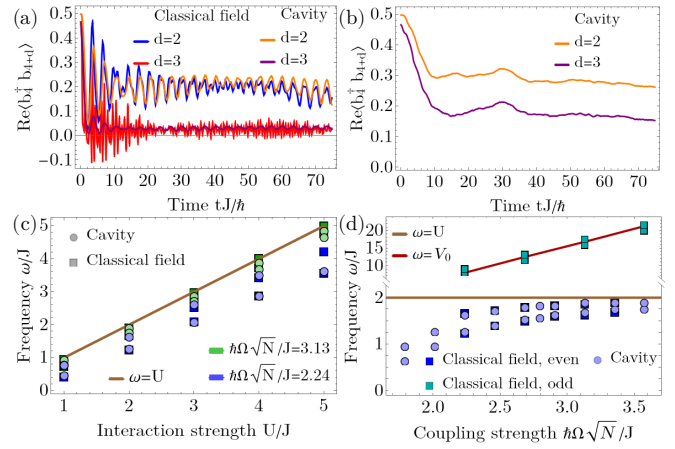


FIG. 4: (a)-(b) Time evolution of the single particle correlations $\text{Re}\langle b_1^\dagger b_{4+d} \rangle$ (a) for a strong coupling $\hbar\Omega\sqrt{N}/J = 3.35$, (b) for weak $\hbar\Omega\sqrt{N}/J = 1.72$ and $U/J = 2$, $L = 14$, $N = 7$, $\hbar\Gamma/J = 1$, $\hbar\delta/J = 2$ (c)-(d) Frequencies extracted from the dynamics of single particle correlations as a function of U and Ω . The lines at $\omega = U$ (brown) and $\omega = V_0$ (dark red) represent the expectation for the collapse and revival dynamics for a deep superlattice, where $V_0 = V(t \approx 75)$.

$\hbar\delta/J = 2$, $U/J = 2$. In this situation, it is much harder to obtain analytical insights or track individual eigenvalues in the ED spectrum, however the numerical tMPS methods allow for simulations up to long times, Fig. 4.

The results show that at strong atoms-cavity coupling, deep in the self-organized phase [55, 56], we observe very similar synchronized oscillations in the single particle correlations at even distances as before, surviving up to very long times, Fig. 4(a). In contrast, for a coupling close to the self-organization threshold the oscillations are absent, Fig. 4(b). In order to verify that the synchronized oscillations occurring in this regime are induced by coherences between states with different interaction energies, we look at the scaling of their frequency with U , Fig. 4(b). We obtain the expected linear scaling with U as for the ED results in Fig. 1(e) in the regime of small J . Furthermore, as we go deeper into the self-organized phase by increasing $\hbar\Omega\sqrt{N}/J$, the higher value of the two frequencies approaches the value of the interaction U , as shown in Fig. 4(d). This implies that the states with coherences between configurations with the same imbalance, but different interaction energies, are long lived metastable states and produce the oscillations observed. For large Ω the atoms feel a strong self-organized potential, which by suppressing the atomic kinetic energy gives rise to an emergent approximate strong symmetry, similar to the one we discussed for small J . In contrast to the small J case, in this situation a similar synchronized oscillatory behavior and dependence of the frequencies is recovered from the simulations in a classical potential (Fig. 4(a),(c),(d)) and the single particle correlations at odd distances are not suppressed to such a small value as before, Fig. 4(a). After an initial decay the correlations satu-

rate to a finite value comparable to the value obtained in the classical potential. However, in the classical potential the correlations at odd distances exhibits the oscillations induced by the height of the potential (upper part of Fig. 4(d)), not present for the coupling to the cavity.

Conclusions: We investigated how the dynamical properties of interacting atoms confined to a one-dimensional chain can be controlled by the coupling to the quantum field of a dissipative optical cavity. We show that by engineering the coupling to the cavity the dynamics of atomic correlations strongly depends on the distance between the sites they probe. In particular, for the single particle correlations at even distances we recover a dissipative analog of the collapse and revival coherence behavior, exhibiting metastable synchronization, i.e. an oscillatory evolution up to long times, with the frequency set by the atomic interactions. In contrast, the coherences at odd distances are strongly suppressed on short times, with the timescales set by the cavity parameters and atoms-cavity coupling strength. Important insights are obtained by considering the approximate strong symmetries of the open coupled atoms-cavity system. The suppression of the odd correlations stems from the fact that they probe subspaces of the Liouvillian with large decay rates, while the dynamics of even correlations is contained close to the decoherence free subspace protected by the symmetry. This offers the opportunity to induce non-trivial dynamical behavior in other many-body dissipative quantum systems. We further show that the approximate symmetry can arise dynamically in self-organized regime. Experimentally, the synchronized collapse and revival dynamics of the coherences would be visible in the momentum distribution obtained in time-of-flight measurements [26]. However, the momentum occupations have contributions from both the even and odd single particle correlations, thus, to probe their very different time-evolution in-situ coherence measurements would be needed.

Data availability: The supporting data for this article are openly available at Zenodo [63].

Acknowledgments: We thank J.P. Brantut, T. Donner, T. Giamarchi, S. Jäger, H. Ritsch, L. Tolle, and C. Waechtler for fruitful discussions. We acknowledge support by the Swiss National Science Foundation under Division II grants 200020-188687 and 200020-219400 and by the Deutsche Forschungsgemeinschaft (DFG, German Research Foundation) under project number 277625399 - TRR 185 (B4), project number 277146847 - CRC 1238 (C05), project number 429529648 - CRC-TRR 306 "QuCoLiMa", and under Germany's Excellence Strategy – Cluster of Excellence Matter and Light for Quantum Computing (ML4Q) EXC 2004/1 – 390534769. This research was supported in part by the National Science Foundation under Grants No. NSF PHY-1748958 and PHY-2309135.

- [1] S. Diehl, A. Micheli, A. Kantian, B. Kraus, H. P. Büchler, and P. Zoller, *Quantum states and phases in driven open quantum systems with cold atoms*, *Nature Physics* **4**, 878 (2008).
- [2] F. Verstraete, M. M. Wolf, and J. Ignacio Cirac, *Quantum computation and quantum-state engineering driven by dissipation*, *Nature Physics* **5**, 633 (2009).
- [3] M. Müller, S. Diehl, G. Pupillo, and P. Zoller, *Engineered Open Systems and Quantum Simulations with Atoms and Ions*, *Advances in Atomic, Molecular, and Optical Physics*, *Advances In Atomic, Molecular, and Optical Physics*, **61**, 1 (2012).
- [4] H. M. Wiseman and G. J. Milburn, *Quantum Measurement and Control* (Cambridge University Press, 2009).
- [5] J. Zhang, Y. xi Liu, R.-B. Wu, K. Jacobs, and F. Nori, *Quantum feedback: Theory, experiments, and applications*, *Physics Reports* **679**, 1 (2017).
- [6] C.-E. Bardyn, M. A. Baranov, C. V. Kraus, E. Rico, A. Imamoglu, P. Zoller, and S. Diehl, *Topology by dissipation*, *New Journal of Physics* **15**, 085001 (2013).
- [7] G. T. Landi, D. Poletti, and G. Schaller, *Nonequilibrium boundary-driven quantum systems: Models, methods, and properties*, *Rev. Mod. Phys.* **94**, 045006 (2022).
- [8] F. Mivehvar, H. Ritsch, and F. Piazza, *Cavity-Quantum-Electrodynamical Toolbox for Quantum Magnetism*, *Phys. Rev. Lett.* **122**, 113603 (2019).
- [9] S. Ostermann, H.-W. Lau, H. Ritsch, and F. Mivehvar, *Cavity-induced emergent topological spin textures in a Bose-Einstein condensate*, *New Journal of Physics* **21**, 013029 (2019).
- [10] N. Masalaeva, W. Niedenzu, F. Mivehvar, and H. Ritsch, *Spin and density self-ordering in dynamic polarization gradients fields*, *Phys. Rev. Res.* **3**, 013173 (2021).
- [11] A. Chiochetta, D. Kiese, C. P. Zelle, F. Piazza, and S. Diehl, *Cavity-induced quantum spin liquids*, *Nature Communications* **12**, 5901 (2021).
- [12] P. Urich, S. Bandyopadhyay, N. Sauerwein, J. Sonner, J.-P. Brantut, and P. Hauke, *A cavity quantum electrodynamics implementation of the Sachdev-Ye-Kitaev model* (2023), arXiv:2303.11343 [quant-ph].
- [13] C. Kollath, A. Sheikhan, S. Wolff, and F. Brennecke, *Ultracold Fermions in a Cavity-Induced Artificial Magnetic Field*, *Phys. Rev. Lett.* **116**, 060401 (2016).
- [14] A. Sheikhan, F. Brennecke, and C. Kollath, *Cavity-induced generation of nontrivial topological states in a two-dimensional Fermi gas*, *Phys. Rev. A* **94**, 061603 (2016).
- [15] K. E. Ballantine, B. L. Lev, and J. Keeling, *Meissner-like Effect for a Synthetic Gauge Field in Multimode Cavity QED*, *Phys. Rev. Lett.* **118**, 045302 (2017).
- [16] C.-M. Halati, A. Sheikhan, and C. Kollath, *Cavity-induced artificial gauge field in a Bose-Hubbard ladder*, *Phys. Rev. A* **96**, 063621 (2017).
- [17] F. Mivehvar, H. Ritsch, and F. Piazza, *Superradiant Topological Peierls Insulator inside an Optical Cavity*, *Phys. Rev. Lett.* **118**, 073602 (2017).
- [18] E. Colella, F. Mivehvar, F. Piazza, and H. Ritsch, *Hofstadter butterfly in a cavity-induced dynamic synthetic magnetic field*, *Phys. Rev. B* **100**, 224306 (2019).
- [19] B. Sciola, D. Poletti, and C. Kollath, *Two-Time Correlations Probing the Dynamics of Dissipative Many-Body Quantum Systems: Aging and Fast Relaxation*, *Phys. Rev. Lett.* **114**, 170401 (2015).
- [20] W. Yi, S. Diehl, A. J. Daley, and P. Zoller, *Driven-dissipative many-body pairing states for cold fermionic atoms in an optical*

- lattice, *New Journal of Physics* **14**, 055002 (2012).
- [21] T. Kinoshita, T. Wenger, and D. S. Weiss, *A quantum Newton's cradle*, *Nature* **440**, 900 (2006).
- [22] I. Bloch, J. Dalibard, and W. Zwerger, *Many-body physics with ultracold gases*, *Rev. Mod. Phys.* **80**, 885 (2008).
- [23] M. Cheneau, P. Barmettler, D. Poletti, M. Endres, P. Schauß, T. Fukuhara, C. Gross, I. Bloch, C. Kollath, and S. Kuhr, *Light-cone-like spreading of correlations in a quantum many-body system*, *Nature* **481**, 484 (2012).
- [24] M. Gring, M. Kuhnert, T. Langen, T. Kitagawa, B. Rauer, M. Schreitl, I. Mazets, D. A. Smith, E. Demler, and J. Schmiedmayer, *Relaxation and Prethermalization in an Isolated Quantum System*, *Science* **337**, 1318 (2012).
- [25] S. Trotzky, Y.-A. Chen, A. Flesch, I. P. McCulloch, U. Schollwöck, J. Eisert, and I. Bloch, *Probing the relaxation towards equilibrium in an isolated strongly correlated one-dimensional Bose gas*, *Nature Physics* **8**, 325 (2012).
- [26] M. Greiner, O. Mandel, T. W. Hänsch, and I. Bloch, *Collapse and revival of the matter wave field of a Bose–Einstein condensate*, *Nature* **419**, 51 (2002).
- [27] A. Eckardt and E. Anisimovas, *High-frequency approximation for periodically driven quantum systems from a Floquet-space perspective*, *New Journal of Physics* **17**, 093039 (2015).
- [28] M. Holthaus, *Floquet engineering with quasienergy bands of periodically driven optical lattices*, *Journal of Physics B: Atomic, Molecular and Optical Physics* **49**, 013001 (2015).
- [29] J. Zhang, P. W. Hess, A. Kyprianidis, P. Becker, A. Lee, J. Smith, G. Pagano, I.-D. Potirniche, A. C. Potter, A. Vishwanath, N. Y. Yao, and C. Monroe, *Observation of a discrete time crystal*, *Nature* **543**, 217 (2017).
- [30] S. Choi, J. Choi, R. Landig, G. Kucsko, H. Zhou, J. Isoya, F. Jelezko, S. Onoda, H. Sumiya, V. Khemani, C. von Keyserlingk, N. Y. Yao, E. Demler, and M. D. Lukin, *Observation of discrete time-crystalline order in a disordered dipolar many-body system*, *Nature* **543**, 221 (2017).
- [31] H. Keßler, P. Kongkhambut, C. Georges, L. Mathey, J. G. Cosme, and A. Hemmerich, *Observation of a Dissipative Time Crystal*, *Phys. Rev. Lett.* **127**, 043602 (2021).
- [32] P. Kongkhambut, J. Skulte, L. Mathey, J. G. Cosme, A. Hemmerich, and H. Keßler, *Observation of a continuous time crystal*, *Science* **377**, 670 (2022).
- [33] V. V. Albert and L. Jiang, *Symmetries and conserved quantities in Lindblad master equations*, *Phys. Rev. A* **89**, 022118 (2014).
- [34] B. Buča, J. Tindall, and D. Jaksch, *Non-stationary coherent quantum many-body dynamics through dissipation*, *Nature Communications* **10**, 1730 (2019).
- [35] B. Buča, C. Booker, and D. Jaksch, *Algebraic theory of quantum synchronization and limit cycles under dissipation*, *SciPost Phys.* **12**, 097 (2022).
- [36] B. Buča and T. Prosen, *A note on symmetry reductions of the Lindblad equation: transport in constrained open spin chains*, *New Journal of Physics* **14**, 073007 (2012).
- [37] C.-M. Halati, A. Sheikhan, and C. Kollath, *Breaking strong symmetries in dissipative quantum systems: Bosonic atoms coupled to a cavity*, *Phys. Rev. Research* **4**, L012015 (2022).
- [38] H. Carmichael, *An open systems approach to quantum optics* (Springer Verlag, Berlin Heidelberg, 1991).
- [39] H. P. Breuer and F. Petruccione, *The theory of open quantum systems* (Oxford University Press, Oxford, 2002).
- [40] C. Maschler, I. B. Mekhov, and H. Ritsch, *Ultracold atoms in optical lattices generated by quantized light fields*, *The European Physical Journal D* **46**, 545 (2008).
- [41] H. Ritsch, P. Domokos, F. Brennecke, and T. Esslinger, *Cold atoms in cavity-generated dynamical optical potentials*, *Rev. Mod. Phys.* **85**, 553 (2013).
- [42] F. Mivehvar, F. Piazza, T. Donner, and H. Ritsch, *Cavity QED with quantum gases: new paradigms in many-body physics*, *Advances in Physics* **70**, 1 (2021).
- [43] J. Klinder, H. Keßler, M. R. Bakhtiari, M. Thorwart, and A. Hemmerich, *Observation of a Superradiant Mott Insulator in the Dicke-Hubbard Model*, *Phys. Rev. Lett.* **115**, 230403 (2015).
- [44] R. Landig, L. Hruby, N. Dogra, M. Landini, R. Mottl, T. Donner, and T. Esslinger, *Quantum phases from competing short- and long-range interactions in an optical lattice*, *Nature* **532**, 476 (2016), letter.
- [45] L. Hruby, N. Dogra, M. Landini, T. Donner, and T. Esslinger, *Metastability and avalanche dynamics in strongly correlated gases with long-range interactions*, *Proceedings of the National Academy of Sciences* **115**, 3279 (2018).
- [46] W. Niedenzu, R. Schulze, A. Vukics, and H. Ritsch, *Microscopic dynamics of ultracold particles in a ring-cavity optical lattice*, *Phys. Rev. A* **82**, 043605 (2010).
- [47] A. O. Silver, M. Hohenadler, M. J. Bhaseen, and B. D. Simons, *Bose-Hubbard models coupled to cavity light fields*, *Phys. Rev. A* **81**, 023617 (2010).
- [48] S. Fernández-Vidal, G. De Chiara, J. Larson, and G. Morigi, *Quantum ground state of self-organized atomic crystals in optical resonators*, *Phys. Rev. A* **81**, 043407 (2010).
- [49] Y. Li, L. He, and W. Hofstetter, *Lattice-supersolid phase of strongly correlated bosons in an optical cavity*, *Phys. Rev. A* **87**, 051604 (2013).
- [50] M. R. Bakhtiari, A. Hemmerich, H. Ritsch, and M. Thorwart, *Nonequilibrium Phase Transition of Interacting Bosons in an Intra-Cavity Optical Lattice*, *Phys. Rev. Lett.* **114**, 123601 (2015).
- [51] T. Flottat, L. d. F. de Parny, F. Hébert, V. G. Rousseau, and G. G. Batrouni, *Phase diagram of bosons in a two-dimensional optical lattice with infinite-range cavity-mediated interactions*, *Phys. Rev. B* **95**, 144501 (2017).
- [52] E. I. Rodríguez Chiacchio and A. Nunnenkamp, *Tuning the relaxation dynamics of ultracold atoms in a lattice with an optical cavity*, *Phys. Rev. A* **97**, 033618 (2018).
- [53] R. Lin, L. Papariello, P. Molognini, R. Chitra, and A. U. J. Lode, *Superfluid-Mott-insulator transition of ultracold superradiant bosons in a cavity*, *Phys. Rev. A* **100**, 013611 (2019).
- [54] L. Himbert, C. Cormick, R. Kraus, S. Sharma, and G. Morigi, *Mean-field phase diagram of the extended Bose-Hubbard model of many-body cavity quantum electrodynamics*, *Phys. Rev. A* **99**, 043633 (2019).
- [55] C.-M. Halati, A. Sheikhan, H. Ritsch, and C. Kollath, *Numerically Exact Treatment of Many-Body Self-Organization in a Cavity*, *Phys. Rev. Lett.* **125**, 093604 (2020).
- [56] A. V. Bezvershenko, C.-M. Halati, A. Sheikhan, C. Kollath, and A. Rosch, *Dicke Transition in Open Many-Body Systems Determined by Fluctuation Effects*, *Phys. Rev. Lett.* **127**, 173606 (2021).
- [57] S. Sharma, S. B. Jäger, R. Kraus, T. Roscilde, and G. Morigi, *Quantum Critical Behavior of Entanglement in Lattice Bosons with Cavity-Mediated Long-Range Interactions*, *Phys. Rev. Lett.* **129**, 143001 (2022).
- [58] T. Chanda, R. Kraus, J. Zakrzewski, and G. Morigi, *Bond order via cavity-mediated interactions*, *Phys. Rev. B* **106**, 075137 (2022).
- [59] See Supplemental Material regarding the details on the time-dependent matrix product states approach (tMPS), the model we consider in the case of a classical superlattice potential, the analytical derivations of the eigenvalues and eigenstates of the

Liouvillian in the limit of vanishing hopping, and the dynamics of quantum trajectories. The Supplemental Material includes Refs. [64–75]

- [60] C.-M. Halati, A. Sheikhan, and C. Kollath, *Theoretical methods to treat a single dissipative bosonic mode coupled globally to an interacting many-body system*, *Phys. Rev. Research* **2**, 043255 (2020).
- [61] C. Sánchez Muñoz, B. Buča, J. Tindall, A. González-Tudela, D. Jaksch, and D. Porras, *Symmetries and conservation laws in quantum trajectories: Dissipative freezing*, *Phys. Rev. A* **100**, 042113 (2019).
- [62] J. Tindall, D. Jaksch, and C. S. Muñoz, *On the generality of symmetry breaking and dissipative freezing in quantum trajectories*, *SciPost Phys. Core* **6**, 004 (2023).
- [63] C.-M. Halati, A. Sheikhan, G. Morigi, and C. Kollath, (2024). Figure data for article "Controlling the dynamics of atomic correlations via the coupling to a dissipative cavity" [Data set]. Zenodo. [10.5281/zenodo.10890066](https://doi.org/10.5281/zenodo.10890066)
- [64] C.-M. Halati, *External Control of Many-Body Quantum Systems*, *Ph.D. thesis*, University of Bonn (2021).
- [65] J. Dalibard, Y. Castin, and K. Mølmer, *Wave-function approach to dissipative processes in quantum optics*, *Phys. Rev. Lett.* **68**, 580 (1992).
- [66] C. W. Gardiner, A. S. Parkins, and P. Zoller, *Wave-function quantum stochastic differential equations and quantum-jump simulation methods*, *Phys. Rev. A* **46**, 4363 (1992).
- [67] A. J. Daley, *Quantum trajectories and open many-body quantum systems*, *Advances in Physics* **63**, 77 (2014).
- [68] S. R. White and A. E. Feiguin, *Real-Time Evolution Using the Density Matrix Renormalization Group*, *Phys. Rev. Lett.* **93**, 076401 (2004).
- [69] A. J. Daley, C. Kollath, U. Schollwöck, and G. Vidal, *Time-dependent density-matrix renormalization-group using adaptive effective Hilbert spaces*, *Journal of Statistical Mechanics: Theory and Experiment* **2004**, P04005 (2004).
- [70] U. Schollwöck, *The density-matrix renormalization group in the age of matrix product states*, *Annals of Physics* **326**, 96 (2011).
- [71] E. M. Stoudenmire and S. R. White, *Minimally entangled typical thermal state algorithms*, *New Journal of Physics* **12**, 055026 (2010).
- [72] M. L. Wall, A. Safavi-Naini, and A. M. Rey, *Simulating generic spin-boson models with matrix product states*, *Phys. Rev. A* **94**, 053637 (2016).
- [73] M. Fishman, S. R. White, and E. M. Stoudenmire, *The ITensor Software Library for Tensor Network Calculations*, *SciPost Phys. Codebases*, 4 (2022).
- [74] D. Nagy, G. Szirmai, and P. Domokos, *Self-organization of a Bose-Einstein condensate in an optical cavity*, *The European Physical Journal D* **48**, 127 (2008).
- [75] D. Poletti, P. Barmettler, A. Georges, and C. Kollath, *Emergence of Glasslike Dynamics for Dissipative and Strongly Interacting Bosons*, *Phys. Rev. Lett.* **111**, 195301 (2013).

SUPPLEMENTAL MATERIAL

Time-dependent matrix product states method for open cavity-atoms systems

The numerically exact results for the time evolution of the Liouvillian, Eqs. (1)-(2) in the main text, describing a one-dimensional Bose-Hubbard model coupled to the dissipative cavity, are obtained with a recent implementation of a matrix product states (MPS) method [55, 60, 64]. The method has been developed to perform the time-evolution of cavity-atoms coupled dissipative systems and the details regarding the implementation and benchmarks are presented in Ref. [60]. This approach employs the stochastic unravelling of the master equation with quantum trajectories [65–67] and a variant of the quasi-exact time-dependent variational matrix product state (tMPS) based on the Trotter-Suzuki decomposition of the time evolution propagator [68–70] and the dynamical deformation of the MPS structure using swap gates [70–72]. Our implementation makes use of the ITensor Library [73].

The convergence of our results is sufficient for at least 500 quantum trajectories in the Monte Carlo sampling. The other convergence parameters are chosen as described in the following: for the results presented in Fig. 2 and Fig. 3 of the main text we use a maximal bond dimension of 100 states, which ensured a truncation error of at most 10^{-7} , the time-step used was $dtJ/\hbar = 10^{-5}$, and the adaptive cutoff of the local Hilbert space of the photonic mode ranged between $N_{\text{pho}} = 40$ and $N_{\text{pho}} = 8$; for the results presented in Fig. 4 of the main text we use a maximal bond dimension of 300 states, which ensured a truncation error of at most 10^{-7} , the time-step used was $dtJ/\hbar = 0.0125$, and adaptive cutoff of the local Hilbert space of the photonic mode between $N_{\text{pho}} = 45$ and $N_{\text{pho}} = 15$.

Dynamics of the Bose-Hubbard in a classical cavity field potential

In the main text we contrast the dynamics of single-particle correlations of the Bose-Hubbard model coupled to the quantum dissipative field of an optical cavity with results of a closed system in which the interacting bosons are subject to a superlattice staggered potential. In the latter case, the staggered potential can be derived as a mean-field description of the cavity-atoms coupling, approach in which the cavity field is described by a classical coherent field [40, 41, 74]. Within this approximation the atoms are described by the Hamilto-

nian

$$\begin{aligned}
H_{\text{MF}} &= H_{\text{int}} + H_{\text{kin}} + H_{\text{stag}} \quad (\text{B.1}) \\
H_{\text{int}} &= \frac{U}{2} \sum_{j=1}^L n_j (n_j - 1), \\
H_{\text{kin}} &= -J \sum_{j=1}^{L-1} (b_j^\dagger b_{j+1} + b_{j+1}^\dagger b_j), \\
H_{\text{stag}} &= -V(t)\Delta, \quad \Delta = \sum_{j=1}^L (-1)^j n_j,
\end{aligned}$$

where $V(t)$ mimics the coupling to a classical cavity field described by a time-dependent coherent state. For the purpose of the comparison performed in the main text regarding the behavior of the atomic correlations, we derive $V(t)$ from exact time-dependence of the photon number via the mean-field relation

$$V_{\text{exact}}(t) = \frac{2\hbar\delta\Omega}{\sqrt{\delta^2 + \Gamma^2/4}} \sqrt{\langle a^\dagger a \rangle_{\text{exact}}(t)}, \quad (\text{B.2})$$

where $\langle a^\dagger a \rangle_{\text{exact}}(t)$ is given by the full model, Eqs. (1)-(2) in the main text, for example shown in Fig. 3 of the main text. This choice allows for a comparison between a quantum dissipative and classical potentials, which contain the same time-scales and average behavior, thus, pinpointing the role of the nature of the dissipation and fluctuation effects stemming from the cavity-atoms coupling.

As in the effective Hamiltonian given in Eq. (B.1) we impose the sign of the classical potential coupled to the atomic imbalance, we break the \mathbb{Z}_2 weak symmetry found in the full Liouvillian (Eqs. (1)-(2) in the main text) associated to changing the sign of the cavity field. Thus, in order to be able to compare the results between the exact evolution and the mean-field approach we perform the time evolution with both signs $H_{\text{stag}} = \pm V(t)\Delta$ and average the results to describe a mixture of states with the two possible signs of the imbalance and recover the \mathbb{Z}_2 symmetry.

Symmetries and Liouvillian spectrum for vanishing hopping

$$J = 0$$

In the first part of the main text we consider parameter regimes in which a separation of scales exists between the parameters describing the cavity field and the ones corresponding to the atoms, $\hbar\Gamma, \hbar\Omega, \hbar\delta \gg J$. Thus, it is useful to get an intuition regarding the spectrum of the Liouvillian in the limit of vanishing hopping, $J = 0$,

$$\mathcal{L}_0(\cdot) = -\frac{i}{\hbar} [H_c + H_{\text{int}} + H_{\text{ac}}, \cdot] + \mathcal{D}(\cdot). \quad (\text{C.1})$$

In this limit we can analytically compute the eigenstates and eigenvalues of \mathcal{L}_0 . We can observe that in \mathcal{L}_0 all atomic operators are diagonal in the position basis due to a strong symmetry [33, 36]. For an open quantum system to have a strong

symmetry, the generators of the symmetry need to commute with both the Hamiltonian and the jump operators, which in our case are the local atomic density operators.

We can block diagonalize the Liouvillian into symmetry sectors of the form $|pho; \{n_j\}\rangle \langle pho', \{n'_j\}|$, where the atomic states are fully characterized by the densities distributions $\{n_j\}$ and $\{n'_j\}$, and the photonic states $|pho\rangle$ and $\langle pho'|$ need to be determined. Only for the case that $\{n_j\}$ and $\{n'_j\}$ are identical, the sector contains a physical steady state, otherwise the sector only consists of traceless states.

In the following, we discuss some eigenstates of \mathcal{L}_0 and their corresponding right eigenvalues for $J = 0$ in more detail. The steady states, which have an eigenvalue $\lambda_{0,\text{st}} = 0$ are given by

$$\rho_{0,\text{st}} = |\alpha(\Delta); \{n_j\}\rangle \langle \alpha(\Delta); \{n_j\}|, \quad (\text{C.2})$$

with the atomic part diagonal in the Fock space, with the local densities $\{n_j\}$ parameterizing the symmetry sector. The photons are in a coherent state which depends on the atomic imbalance $\alpha(\Delta) = \frac{\Omega}{\delta - i\Gamma/2} \Delta$, with $\Delta = \sum_j (-1)^j n_j$. One can find excited eigenstates in these sectors by creating photon excitations on top of the coherent state, for example in the subspace of single photon excitations P_1 , we have

$$\rho_{P_1} = [a^\dagger - \alpha(\Delta)^*] |\alpha(\Delta); \{n_j\}\rangle \langle \alpha(\Delta); \{n_j\}|, \quad (\text{C.3})$$

with

$$\lambda_{P_1} = -\frac{\hbar\Gamma}{2} - i\hbar\delta. \quad (\text{C.4})$$

One can show that ρ_{P_1} is an eigenstate by performing a displacement of the photonic operators with the value $\alpha(\Delta)$. Furthermore, a harmonic oscillator ladder is obtained with the creation ladder operators given by $a^\dagger - \alpha(\Delta)^*$ generating multi-photon excitations. Thus, the eigenvalues corresponding to these multi-photon excitations will have a real part spaced by integer multiples of $-\hbar\Gamma/2$. We note that the adjoint state $\rho_{P_1}^\dagger$ is also an eigenstate with the eigenvalue $\lambda_{P_1}^*$.

Next, one can show that states that are not diagonal in the atomic part, of the form $|\alpha(\Delta); \{n_j\}\rangle \langle \alpha(\Delta'); \{n'_j\}|$ are eigenstates with the eigenvalues

$$\begin{aligned}
\lambda(\Delta, u, \Delta', u') &= -\frac{1}{2} \frac{\hbar\Omega^2\Gamma}{\delta^2 + \Gamma^2/4} (\Delta - \Delta')^2 \quad (\text{C.5}) \\
&+ i \left[\frac{\hbar\Omega^2\delta}{\delta^2 + \Gamma^2/4} (\Delta^2 - \Delta'^2) - (u - u') \right],
\end{aligned}$$

with the odd-even imbalances, $\Delta = \sum_j (-1)^j n_j$ and $\Delta' = \sum_j (-1)^j n'_j$ and the total interaction energies $u = \frac{U}{2} \sum_j n_j (n_j - 1)$ and $u' = \frac{U}{2} \sum_j n'_j (n'_j - 1)$. Based on the values of the imbalances and interaction energies we can identify the following cases:

- For $\Delta = \Delta'$, even for different density distributions $\{n_j\}$ and $\{n'_j\}$, the states

$$\rho_0 = |\alpha(\Delta); \{n_j\}\rangle \langle \alpha(\Delta); \{n'_j\}|, \quad (\text{C.6})$$

have eigenvalues with vanishing real part

$$\lambda_0 = -i(u - u'). \quad (\text{C.7})$$

In the case $u = u'$ we have traceless states with $\lambda_0 = 0$, showing the existence of off-diagonal coherences between Fock states that can survive in the steady states. Alternatively, for $u \neq u'$, we obtain states with purely imaginary eigenvalues. These states, called rotating coherences [33], can lead to persistent synchronized oscillations in the long time limit [34, 35].

The evolution of some of these states can be probed by monitoring, for example, the evolution of single particle correlations at even distances $b_j^\dagger b_{j+2d}$ [34, 35], as they probe the coherences induced by states which have the same imbalance Δ in the bra and the ket contribution.

Furthermore, as shown in Ref. [34, 35], we can use the operators $b_i^\dagger b_{i+2d}$ to construct the states with purely imaginary eigenvalues. As the following conditions are fulfilled

$$\begin{aligned} [H_c + H_{\text{int}} + H_{\text{ac}}, b_i^\dagger b_{i+2d}] \rho_{0,st} &= \\ &= -U(n_{i+2d} - 1 - n_i) b_i^\dagger b_{i+2d} \rho_{0,st}, \\ [a, b_i^\dagger b_{i+2d}] \rho_{0,st} &= 0, \end{aligned} \quad (\text{C.8})$$

then the state $b_j^\dagger b_{j+2d} \rho_{0,st}$ is an eigenstate of the Liouvillian \mathcal{L}_0 with the eigenvalue $-U(n_{j+2d} - 1 - n_j)i$. Thus, we recover a subset of the states given in Eq. (C.6). We note that in Eq. (C.8) we made use in the calculation that $\rho_{0,st}$ is diagonal in the Fock space.

All the states with a zero real part, Eq. (C.2) and Eq. (C.6), are part of the decoherence free subspace Λ_0 (see Fig. 1 in the main text).

- For $\Delta \neq \Delta'$ we observe in Eq. (C.5) that the real part of the eigenvalues is finite and proportional to $(\Delta - \Delta')^2$. Thus, the states with the lowest decaying rate are the ones for which $\Delta' = \Delta \pm 2$, which we mark by the subspace Λ_1 in Fig. 1 in the main text,

$$\rho_1 = |\alpha(\Delta); \{n_j\}\rangle \langle \alpha(\Delta \pm 2); \{n'_j\}|, \quad (\text{C.9})$$

corresponding to the eigenvalues

$$\begin{aligned} \lambda_1(\Delta, u, \Delta \pm 2, u') &= -\frac{2\hbar\Omega^2\Gamma}{\delta^2 + \Gamma^2/4} \\ &- i \left[\frac{4\hbar\Omega^2\delta}{\delta^2 + \Gamma^2/4} (1 \pm \Delta) + (u - u') \right]. \end{aligned} \quad (\text{C.10})$$

Depending on the initial state, the decay of such states can be observed in the evolution of the single particle correlations at odd distances $b_j^\dagger b_{j+2d+1}$.

We note that a similar construction as in Eq. (C.3) is possible to describe the photonic excitations in the symmetry sectors in which the lowest decaying states are given by the ones of Eq. (C.6) and Eq. (C.9).

Furthermore, with the knowledge of the different dissipative subspaces for $J = 0$ one can compute perturbatively the steady state for finite and small J [19, 60, 75]. Considering the contributions from the subspaces that can be accessed via one hopping event, Λ_1 and back, the effective dynamics for the elements of the decoherence free subspace is given by

$$\frac{\partial}{\partial t} \rho_0 = \lambda_0 \rho_0 + \frac{1}{\hbar^2} X_0 [H_{\text{kin}}, \mathcal{L}_0^{-1} X_1 [H_{\text{kin}}, \rho_0]]. \quad (\text{C.11})$$

The operators X_0 and X_1 are the projectors onto the decoherence free subspace Λ_0 and excited subspace Λ_1 . The kinetic term breaks the strong symmetry of \mathcal{L}_0 , which determines a transition from multiple steady states to a unique steady state given by the mixed state [60, 64]

$$\rho_{\text{mix}} = \frac{1}{\mathcal{N}} \sum_{\{n_j\}} |\alpha(\Delta); \{n_j\}\rangle \langle \alpha(\Delta); \{n_j\}|, \quad (\text{C.12})$$

where the sum runs over all possible density configurations $\{n_j\}$ and \mathcal{N} is the number of these configurations. The state ρ_{mix} exhibits strong, however classical, correlations between the cavity field and the atoms, as for each term in the sum the cavity field is fully determined by the atomic imbalance. By tracing out the photonic states we obtain a fully mixed, infinite temperature, state for the atoms as all density configurations have the same probability.

Dynamics of single quantum trajectories

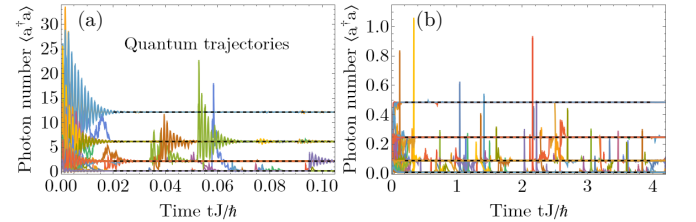


FIG. D1: Time evolution of the photon number for 500 of the sampled quantum trajectories, for the parameters $L = 14$, $N = 7$, $\hbar\delta/J = 5000$, $U/J = 10$, (a) $\hbar\Omega\sqrt{N}/J = 6614$, $\hbar\Gamma/J = 500$, (b) $\hbar\Omega\sqrt{N}/J = 1323$, $\hbar\Gamma/J = 750$. The dashed black lines represent the photon number expected for the possible values of the imbalance $\Delta \in \{\pm 1, \pm 3, \pm 5, \pm 7\}$.

In the presence of a strong symmetry the quantum trajectories obtained in the stochastic unraveling of the master equation can exhibit dissipative freezing [37, 61, 62], i.e. the quantum trajectories can dynamically break the strong symmetry and be projected to just one of the symmetry sectors. This phenomenon occurs when the initial state consists of a superposition of states from different symmetry sectors. The evolution can be sketched as in the following

$$\begin{aligned} |\psi_k(t=0)\rangle &= \sum_{\{n_j\}} c[\{n_j\}] |\{n_j\}\rangle \xrightarrow{\text{projected}} \\ |\psi_k(t \gg 0)\rangle &= |\{n_j\}\rangle \text{ with probability } |c[\{n_j\}]|^2, \end{aligned} \quad (\text{D.1})$$

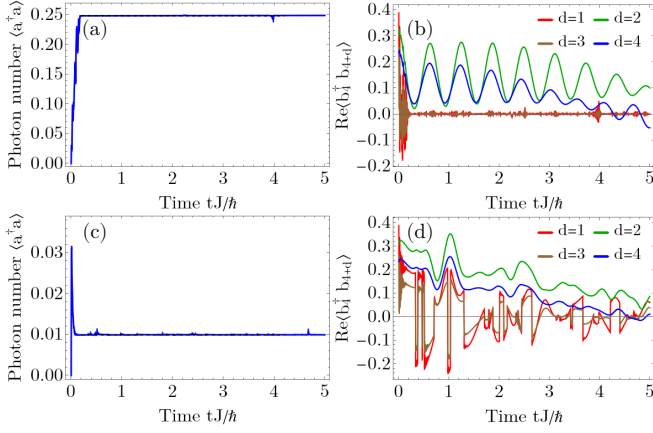


FIG. D2: Time evolution of single quantum trajectories for (a), (c) the photon number and (b), (d) single particle correlations $\text{Re}\langle b_4^\dagger b_{4+d} \rangle$. Panels (a)-(b) correspond to the same trajectory from the subspace $\Delta = \pm 5$, while panels (c)-(d) correspond to a trajectory from the subspace $\Delta = \pm 1$. The parameters used are $L = 14$, $N = 7$, $\hbar\delta/J = 5000$, $U/J = 10$, $\hbar\Omega\sqrt{N}/J = 1323$, $\hbar\Gamma/J = 750$.

where $\{n_j\}$ represents the set of conserved quantities of the symmetry, in our case the local densities, and $c[\{n_j\}]$ the initial amplitudes for each state. We note that in the case in which multiple states with the same values of the conserved quantities exist, the state $|\psi_k(t)\rangle$ can still evolve in time within the symmetry sector. This evolution implies that the steady state of the system is described by a mixed state of the form $\rho_{\text{mix}} = \sum |c[\{n_j\}]|^2 |\{n_j\}\rangle \langle\{n_j\}|$, without any coherences between states from different symmetry sectors. Thus, a necessary condition for dissipative freezing to occur is that no traceless eigenstates with 0 real part of their eigenvalues which correspond to coherences of different symmetry sectors are present [62]. Another exception exists when one has similar symmetry sectors, for which one can find a unitary transformation to map the Hamiltonian of one sector to the Hamiltonian of the other, while only changing the jump operators up to a phase factor [62].

In the case of the system considered here [Eqs. (1)-(2) in the main text] we have shown in the previous section, Eqs. (C.6)-(C.7), that in the limit $J = 0$ states corresponding to coherences between different density configurations, and thus different symmetry sectors, are present in the steady state. Furthermore, we also have similar symmetry sectors for which $n_j = n'_{L+1-j}$ for all $j = 1, \dots, L$. These sectors have an imbalance of opposite signs and can be mapped to each other by the transformation which changes the sign of the jump operator $a \rightarrow -a$. Thus, it is interesting to observe in the dynamics

of quantum trajectories if dissipative freezing can still occur between certain symmetry sectors, while the coherences between others survive to long times.

In Fig. D1 we show the photon number corresponding to single quantum trajectories in the case of small hopping J , which slightly breaks the strong symmetry. However, we have previously shown that also in the presence of an approximate strong symmetry [37], one can still interpret the results in the context of dissipative freezing, as the quantum trajectories are initially projected to the symmetry sectors and only on longer timescales, given by the symmetry breaking term, explore other subspaces. We observe that on short times, $tJ/\hbar \sim 0.02$ in Fig. D1(a) and $tJ/\hbar \sim 0.1$ in Fig. D1(b) all 500 trajectories stabilized to a value of the photon number corresponding to one of the possible values of the imbalance $\Delta \in \{\pm 1, \pm 3, \pm 5, \pm 7\}$. This implies that the quantum trajectories are projected to subspaces spanned by states with the same absolute value of the imbalance. Furthermore by investigating the behavior of the single particle correlations for a trajectory, e.g. corresponding to an imbalance $|\Delta| = 5$ in Fig. D2(b), we can infer that coherences within these subspaces are maintained. We can see that at even distances $\text{Re}\langle b_4^\dagger b_{4+d} \rangle$ exhibits the oscillating dynamics we observed in the Monte Carlo average and discussed in the main text, showing the presence of coherences within the single trajectory. This in contrast to correlations at odd distance which are quickly suppressed and quantify the coherence between sectors with a different $|\Delta|$. The behavior of the odd distance single particle correlations is different for the quantum trajectories which are projected to the symmetry sectors with $\Delta = \pm 1$, Fig. D2(d). As mentioned above $\Delta = 1$ and $\Delta = -1$ are similar symmetry sectors and the coherence between them is not suppressed in the quantum trajectories. Thus, we see in Fig. D2(d) that the correlations at odd distances are finite, however they change sign every time a quantum jump occurs, which leads to a small value in the Monte Carlo average over all the trajectories.

As we consider a finite J we also see in Fig. D1 that rarely there are trajectories that change the subspace of fixed imbalance, capturing the long-time dynamics of approaching the steady state [37].

Thus, we see that the proximity of a strong symmetry of the open system is crucial for the correlation dynamics. The protection of the oscillations present in the single particle correlations at even distances stems from the long lived coherences between degenerate approximate symmetry sectors, while the suppression of the correlations at odd distances is due to the fact that they couple to coherence of distinct symmetry sectors with finite decay rate.